Reid, K. B. M. (1986) *Essays Biochem. 22*, 27–68.
Reid, K. B. M., Bentley, D. R., Campbell, R. D., Chung, L. P., Sim, R. B., Kristensen, T., & Tack, B. F. (1986) *Immunol. Today 7*, 230–234.
Schumaker, V. N., Hanson, D. C., Kilchherr, E., Phillips, M. L., & Poon, P. H. (1986) *Mol. Immunol. 23*, 557–565.
Sim, E., & Sim, R. B. (1983) *Biochem. J. 210*, 567–576.
Sim, E., Dodds, A. W., Wood, M., & Sim, R. B. (1986) *Biochem. Soc. Trans. 14*, 77–78.
Sim, R. B. (1981) *Methods Enzymol. 80*, 26–42.
Sim, R. B., & Sim, E. (1981) *Biochem. J. 193*, 129–141.
Smith, C. A., Vogel, C. W., & Müller-Eberhard, H. J. (1984) *J. Exp. Med. 159*, 324–329.
Tack, B. F., Morris, S. C., & Prahl, J. W. (1979) *Biochemistry 18*, 1497–1505.
Tack, B. F., Janatova, J., Thomas, M. L., Harrison, R. A., & Hammer, C. H. (1981) *Methods Enzymol. 80*, 64–101.
Wetlaufer, A. B. (1962) *Adv. Protein Chem. 17*, 303–390.

Structural Homologies of Component C5 of Human Complement with Components C3 and C4 by Neutron Scattering†

Stephen J. Perkins,*,‡ Kathryn F. Smith,‡ Adam S. Nealis,‡ Peter J. Lachmann,§ and Richard A. Harrison§

Department of Biochemistry and Chemistry and Department of Protein and Molecular Biology, Royal Free Hospital School of Medicine, Rowland Hill Street, London NW3 2PF, U.K., and Molecular Immunopathology Unit, Medical Research Council Centre, Hills Road, Cambridge CB2 2QH, U.K.

Received April 11, 1989; Revised Manuscript Received September 14, 1989

ABSTRACT: The complement component C5 is one of a family of structurally related plasma proteins that includes components C3 and C4. Activation of C5 is the initial step in the formation of the membrane attack complex of complement. Analysis of the solution structure of C5 and comparisons with similar analyses of the structures of C3 and C4 are reported here. Neutron solution scattering gave an M_r for C5 of 201 000, which demonstrates that C5 is monomeric in solution. The radius of gyration R_G of C5 at infinite contrast is 4.87 nm and corresponds to an elongated structure. The longest length of C5 was determined to be at least 15–16 nm from three calculations on the basis of the R_G, the scattering intensity at zero angle $I(0)$, and the indirect transformation of the scattering curve into real space. Comparison of the R_G and contrast variation data and indirect transformations of the scattering curves for C3, C4, and C5 show that these have very similar structures. Comparisons of the C5 scattering curve with Debye small-sphere models previously employed for C4 and C3 show that good curve fits could be obtained. Unlike previous studies that have suggested significant differences, these experiments indicate that, while C5 differs from C3 and C4 in its activation and inactivation pathways, significant structural homology exists between the native proteins, as might be predicted from their high (and similar) sequence homology.

Complement, a multicomponent cascade system found in plasma, plays a major role in the humoral immune system (Reid, 1986). Activation of the early components of the classical and alternative pathways by proteolytic cleavages generates C5 convertase activity. The convertases activate C5 to form C5b and C5a. The generation of C5b is the initial step in the formation of the membrane attack complex, which is assembled from the complement components C6, C7, C8, and C9 in association with C5b. Insertion of the complex into membranes leads to the formation of transmembrane channels in the target cell and ultimately to cell death due to osmotic imbalance.

The primary sequences of the complement components C3, C4, and C5 show significant homologies (Belt et al., 1984; de Bruijn & Fey, 1985; Wetsel et al., 1987, 1988). C5, like C3, is composed of two disulfide-linked polypeptide chains α and β. In contrast, C4 has three chains, α, β, and γ. Activation of C5 is brought about by cleavage of the peptide bond between residues 74 and 75 of the α chain, releasing C5a (Nilsson et al., 1975). C5a is the most potent of the three anaphylatoxins C3a, C4a, and C5a formed by the complement cascade. Despite the sequence homology, the genes for C3, C4, and C5 are found on different chromosomes (Carroll et al., 1984; Whitehead et al., 1982; Wetsel et al., 1988). While not as abundant as C3 and C4, C5 at 0.15 mg/mL is still one of the more abundant complement components in plasma. C3 and C4, but not C5, have a highly reactive internal β-cysteinyl-γ-glutamyl thiolester bond in a region of high sequence homology. During activation, this enables C3b and C4b to form covalent bonds to target surfaces (Law et al., 1980). Since there is no thiolester bond in C5, C5b is unable to form a covalent bond to a surface. Thus, C5b in the presence of C6 forms a fluid-phase C5b6 bimolecular complex, and this in association with C7 expresses a membrane-binding site (Podack et al., 1978).

In this study, comparisons between the solution structures of C3, C4, and C5 are made. Electron microscopy of C5 depicts a multilobal, irregular ultrastructure of dimensions of 10.4 nm × 14.0 nm × 16.8 nm (DiScipio et al., 1983); different

† We thank the Wellcome Trust for support, and the Science and Engineering Research Council for access to the facilities at SRS Daresbury and ILL Grenoble.
* To whom correspondence should be addressed at the Department of Biochemistry and Chemistry.
‡ Royal Free Hospital School of Medicine.
§ Medical Research Council Centre.

0006-2960/90/0429-1175$02.50/0

dimensions have, however, been reported for C3 and C4 (Smith et al., 1982, 1984; Dahlbäck et al., 1983). Limited solution scattering data on C3, C4, and C5 suggested that despite their sequence homologies they had dissimilar R_G values (Österberg et al., 1984, 1988). In this study, extensive neutron scattering experiments on the external and internal structure of C5 are critically compared with similar studies on C3 and C4 (Perkins & Sim, 1986; Perkins et al., 1990). Together, the neutron data show that C3, C4, and C5 are more homologous in their physical structures than previously believed.

Materials and Methods

(*a*) *Sample Preparations.* C5 was prepared from 3.5 L of human plasma from normal, healthy donors essentially as described in Harrison and Lachmann (1986), with the following modifications. Plasma was taken from donors over a period of 2 weeks prior to C5 preparation, EDTA and benzamidine were added to final concentrations of 5 mM, and the plasmas were stored frozen at −70 °C until required. After passage though lysine–Sepharose, the plasma pool was dialyzed [by using a Pellicon ultrafiltration cassette (Millipore) equipped with a 5 ft^2, 10000 nominal molecular weight limit, polysulfone membrane] against 5 mM sodium potassium phosphate, 5 mM EDTA, 5 mM benzamidine, and 50 mM NaCl, pH 7.0, and loaded onto a 10-L DEAE-Sephacel column equilibrated in the same buffer. The protein was eluted with a gradient (25 L each side) to 300 mM NaCl, and C5, eluting early in the gradient, was detected by double diffusion in agarose against a rabbit anti-human C5 antiserum. C5-containing fractions were pooled, concentrated to 150 mL, dialyzed against 20 mM sodium potassium phosphate, 10 mM EDTA, 5 mM benzamidine, and 300 mM NaCl, pH 7.0, and gel-filtered on Sepharose CL-6B (Pharmacia; 6-L column). C5-containing fractions were detected as described above, pooled, and dialyzed against 20 mM sodium potassium phosphate and 100 mM KCl, pH 7.0, before being loaded onto a hydroxylapatite column (Bio-Rad HTP; 600 mL bed volume, 30 × 5.5 cm column) equilibrated in the same buffer. C5 was eluted with a gradient (2.5 L each side) to 2.0 M KCl. Antigenic analysis showed that the small amount of C3 that was contained in the DEAE-Sephacel C5 pool and which cochromatographed with C5 on Sepharose CL-6B was not eluted from hydroxylapatite by KCl. SDS–PAGE analysis showed the C5 to be greater than 95% pure and to have the anticipated two-chain structure. The C5 pool from hydroxylapatite was concentrated to approximately 10 mg/mL and dialyzed against PBS/5 mM sodium azide. Initial neutron scattering studies were performed on freshly prepared C5. Prior to analysis, these were dialyzed against buffer A (see below), filtered through a 0.2-μm filter (ACRO LC13; Gelman Sciences) into 3.0- or 4.8-mL sterile evacuated glass vials (Mallinckrodt Diagnostica Holland B.V., Petten, Holland) and held at 4 °C. Subsequent studies were performed on C5 that had been stored frozen at −70 °C in 1-mL (10 mg) aliquots. These samples were prepared for scattering studies by gel filtration on Sepharose 6B in 12 mM sodium phosphate, 200 mM NaCl, and 1 mM EDTA, pH 7.0. The peak fraction(s) only were reconcentrated to about 10 mg/mL and then dialyzed against the same buffer before (ACRO LC13) filtration and storage as described above. Samples were reanalyzed by SDS–PAGE subsequent to solution scattering studies, and no differences pre- and postscattering were detected.

Four different buffers were used in neutron data collection: A (200 mM NaCl, 12 mM sodium phosphate, 1 mM EDTA, pH 7.0); B (50 mM NaCl, 12 mM sodium phosphate, 1 mM EDTA, pH 7.0); C (3.1 mM diethylbarbituric acid, 0.9 mM sodium barbitone, 145 mM NaCl, 0.83 mM $MgCl_2$, or 0.25 mM $CaCl_2$, 20 μM $ZnSO_4$); D (buffer C diluted 1 in 4, except for $ZnSO_4$, which remained at 20 μM). Buffer A was predominantly used, and dialyses were performed as in Perkins et al. (1990). The composition is calculated from the full 1654-residue sequence of human C5 (Wetsel et al., 1988; R. A. Wetsel, unpublished results). All four putative carbohydrate binding sites at Asn-705, -875, -1079, and -1593 in the human sequence (following the mouse sequence numbering; Wetsel et al., 1987) are occupied with biantennary complex type oligosaccharides, giving a 4.5% oligosaccharide content by mass. DiScipio et al. (1983) reported this content to be 2.7% by mass. The absorption coefficient $A_{280}^{1\%,1cm}$ for human C5 has been estimated as 10.8 (DiScipio et al., 1983) or 10.2 (Österberg et al., 1988), and their mean is used here. Calculation of the absorption coefficient (Perkins, 1986) gives 10.9, in good agreement with DiScipio et al. (1983).

(*b*) *Neutron Scattering Measurements.* Neutron experiments were performed on instrument D17 at the Institut Laue-Langevin, Grenoble, in five independent sessions. Guinier data were obtained by using a sample-to-detector distance of 3.45–3.46 m and wavelengths λ of 1.30–1.60 nm, giving a Q range of 0.0053–0.049 nm^{-1} (where $Q = 4\pi \sin\theta/\lambda$ and 2θ is the scattering angle). Data at larger Q were obtained with a sample-to-detector distance of 1.40 m, a main beam–detector axis angle of 0° or 20°, and wavlengths of 0.99–1.00 nm, giving a Q range of 0.23–3.36 nm^{-1}. Data reduction followed standard procedures (Ghosh, 1981; Perkins et al., 1990). Linear regressions of the match point and Stuhrmann graphs were analyzed by microcomputer using the statistics program MINITAB (version 6.1). The molecular modeling of the C5 neutron curves utilized the methods in Perkins and Weiss (1983), Perkins and Sim (1986), and Perkins et al. (1990).

The use of the indirect transformation procedure (ITP) method (Glatter, 1982) enables the neutron scattering curves $I(Q)$ to be transformed into real space $P(r)$. This calculation requires measurement of the whole scattering curve to large Q, ca. 4 nm^{-1}, and offers an alternative calculation of the radius of gyration R_G and the length L for C5. While 20–25 splines should be used to fit the 75 experimental data points of Figure 4a, only 10 splines were used here because of the limited counting statistics at large Q. The maximum length (which can be up to 50% larger than the expected length L) was specified as 20 nm on the basis of the L calculations from the Guinier R_G analyses; control calculations on the basis of maximum lengths of 17 nm gave similar results. The number of points used to define $P(r)$ in real space was 101.

Results and Discussion

(*a*) *Neutron Scattering Data on C5.* Neutron contrast variation experiments were performed on human C5 at concentrations between 1.8 and 7.9 mg/mL in 0%, 70%, 80%, and 100% ^2H_2O buffers. Linear Guinier analyses were successfully obtained (Figure 1a), from which the intensity $I(0)$ and the radius of gyration R_G were derived in a suitable QR_G range of 0.6–1.5. Linear cross-sectional analyses to obtain $[I(Q)\text{-}Q]_{Q\to 0}$ and R_{XS} values were obtained in the QR_{XS} range 0.7–1.4 (Figure 1b). Buffers A–D were used (Materials and Methods) with ionic strengths of 0.22, 0.07, 0.15, or 0.04 M. The two higher salt buffers A and C did not yield data that differed significantly from the average. In the two lower salt buffers, C5 showed evidence of aggregation, so these data were not considered further. In the higher salt buffers, while the $I(0)/c$ (c is the concentration) and R_G values exhibit minor decreases with concentration (results not shown), this was not

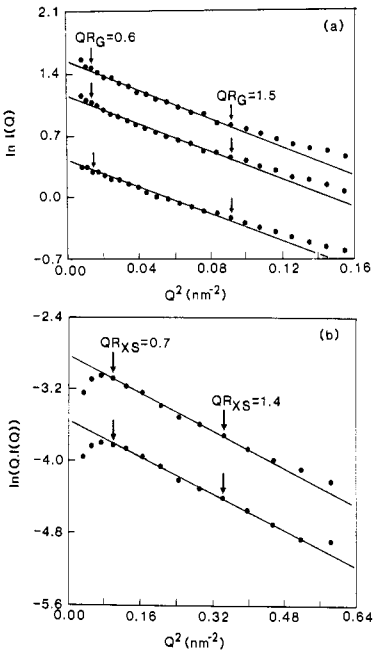

FIGURE 1: Neutron Guinier plots of human complement C5 in 100% ^2H_2O buffers: (a) Guinier plots and (b) cross-sectional Guinier plots of a dilution series for C5. The vertical displacements of the curves reflect sample concentrations at 5.4, 3.9, and 1.9 mg/mL in (a) and 3.9 and 1.9 mg/mL in (b). The R_G fits and QR_G values are reported by using an R_G value of 4.8 nm (Q range of 0.12–0.30 nm^{-1}) and those for QR_{XS} with an R_{XS} value of 2.34 nm (Q range of 0.31–0.58 nm^{-1}). A slight decrease of the R_G with concentration is observable in (a) and in other percent ^2H_2O buffers, but was not significant in terms of the error of the R_{G-C} determination in Table I.

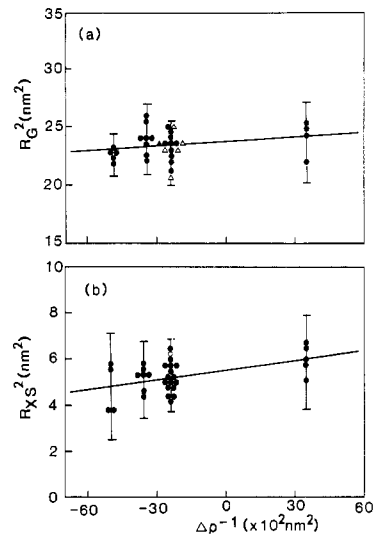

FIGURE 2: Stuhrmann analyses of the contrast variation experiments for human C5. The R_G^2 and R_{XS}^2 data are plotted against the reciprocal solvent–solute contrast difference $\Delta\rho^{-1}$. The symbols correspond to the four buffers used (Materials and Methods) as follows: A, ●; B, ○; C, △; D, ▲. The regressed line based on the R_G^2 values gives an R_C of 4.87 ± 0.03 nm and a slope α of (13 ● 8) × 10^{-5}. For the R_{XS}^2 data, R_C is 2.35 ± 0.03 nm and α is (13 ± 4) × 10^{-5}.

significant, so all the R_G data are given in Figure 2.

Molecular masses M_r were determined from the $I(0)/c$ data for the samples in 0% ^2H_2O in high-salt buffers. The mean of four measurements is 201 000 ± 9000, which is within error of 194 000 calculated from the human C5 sequence (Materials and Methods). This shows that the absorption coefficient of 10.5 used to derive concentrations is satisfactory and that C5 is monomeric in solution. A plot of $[I(0)/ctT_s]^{1/2}$ against volume percent ^2H_2O gives the neutron match point (t is the sample thickness; T_s is the sample transmission). An excellent straight line was obtained, which give a match point of 40.9 ± 0.4% ^2H_2O by linear regression analyses of 33 values in 4 contrasts. The corresponding cross-sectional plot of $[[I(Q)-Q]_{Q\to 0}/ctT_s]^{1/2}$ against percent ^2H_2O yielded a match point of 41.5 ± 0.4% ^2H_2O. Both of these are in reasonable agreement with the match point of 40.6% ^2H_2O predicted (Perkins, 1986) from the human C5 sequence. They support the validity of the R_G and R_{XS} analyses in Figure 2.

Table I: Summary of Guinier Analyses for C5, C4, and C3 of Complement[a]

	C5	C4, C4u, C4(a+b)	C3, C3u, C3(a+b)
X-rays			
R_G (nm)	5.3 ± 0.1	5.3 ± 0.1	5.2 ± 0.1
R_{XS} (nm)	2.3 ± 0.1	2.5 ± 0.1	2.6 ± 0.1
neutrons			
$R_{G\text{-}C}$ (nm)	4.9 ± 0.1	4.9 ± 0.1	5.1 ± 0.1
$R_{XS\text{-}C}$ (nm)	2.4 ± 0.1	2.2 ± 0.1	2.4 ± 0.1
α_G (×10^{-5})	13 ± 8	2 ± 10	30 ± 10
α_{XS} (×10^{-5})	13 ± 4	20 ± 10	10 ± 10

[a] The data for C4 and C3 are taken from Perkins et al. (1990) and Perkins and Sim (1986), and mean values are shown.

To characterize the shape of C5 and its internal structure, the contrast dependence of the structural data was analyzed by using Stuhrmann plots of R_G^2 and R_{XS}^2 against the reciprocal solvent–solute contrast difference $\Delta\rho^{-1}$ (Figure 2). The radii of gyration at infinite contrast $R_{G\text{-}C}$ and $R_{XS\text{-}C}$ were found to be 4.87 and 2.35 nm. The elongation ratio $R_{G\text{-}C}/R_0$ was calculated as 1.61 (where R_0 is the R_G of the shere of the same dry volume as C5: 248 nm^3). This is significantly larger than the value of 1.28 ± 0.10 found in a survey of many globular proteins by X-ray scattering (Perkins, 1988b) and shows that C5 is elongated in shape with one triaxial dimension that is longer than the other two. The radial inhomogeneity of scattering density α is positive at 13 × 10^{-5} in both Stuhrmann plots. This is evidence that C5 has the spatial distribution of amino acids that is typical of soluble globular proteins.

The dimensions of C5 can be calculated from the R_G and R_{XS} data and also from the $I(0)$ and $[I(Q)Q]_{Q\to 0}$ data (Perkins et al., 1990). By use of the data in 100% ^2H_2O, the length L of the longest axis of C5 (assuming an elliptical cylinder) was determined as 14.9 ± 0.5 nm from the R_G and R_{XS} data. From the ratio $\pi I(0)/[I(Q)Q]_{Q\to 0}$, L is found to be 15.7 ± 1.1 nm.

X-ray scattering curves for C5 were obtained by using the synchrotron radiation source at Daresbury (Perkins et al., 1990). In Guinier analyses, the final R_G and R_{XS} values were based on Q ranges of 0.18–0.30 and 0.31–0.60 nm^{-1}, respectively, which are slightly more restricted than those of Figure 1. Only those spectra that could be analyzed by the criteria of linear Guinier plots were used. These resulted in data that were fully consistent within error with those from neutron scattering (Table I).

(b) Comparisons of C5 with C3 and C4 of Complement. Scattering data analyses relating to the presumed homology between C3, C4, and C5 are presented in Table I. The present X-ray and neutron data on C5 are compared with data previously obtained for C3 and C4 and their fragments (Perkins & Sim, 1986; Perkins et al., 1990). C3u and C4u correspond to C3 and C4 with hydrolyzed thiolester bonds, while C3(a+b) and C4(a+b) correspond to activated C3 and C4 in which the two fragments continue to be associated. By both X-ray and neutron scattering, the R_G and R_{XS} values of C3, C3u, C3-(a+b), C4, C4u, C4(a+b), and C5 were found to be the same

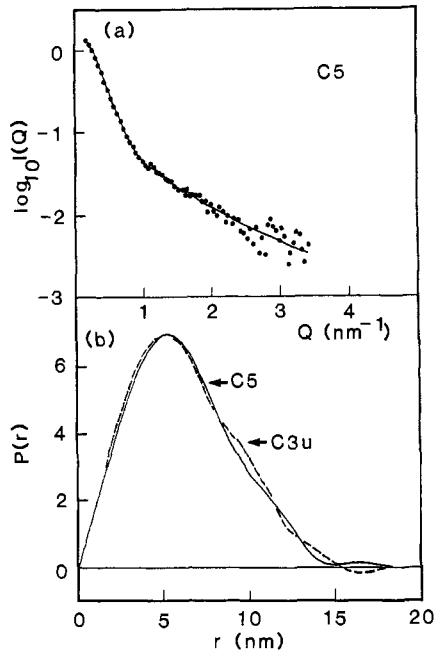

FIGURE 3: Indirect transformation into real space of the C5 and C3u neutron scattering curves in 100% ^2H_2O buffer. (a) The experimental neutron curve of C5 (●) is shown. The continuous line is a polynomial function generated by the ITP program. That for the C3u scattering curve is very similar and is not shown. (b) The intraparticle distance distribution function $P(r)$ for C5 (—) and C3u (---) is shown after normalization for concentration. These were calculated from the curve fits in (a). The $P(r)$ curves for C5 and C3u are seen to be very similar. For C5, a R_G of 4.89 nm was calculated over the range of $-8.0 \leq \lambda_{opt} \leq 0.0$, where λ_{opt} is the Lagrange stabilization parameter used in ITP. For C3u, R_G is 4.77 nm over a similar range of λ_{opt}.

within error (Table I). The R_G values from X-ray scattering correspond to measurements in a positive solute–solvent contrast difference. They are higher than the neutron R_{G-C} values at the infinite contrast condition, thus corroborating the positive Stuhrmann α values obtained from the neutron analyses. It is concluded that C3, C4, and C5 are closely similar in their overall shapes in solution, as judged from the scattering curve analyses out to $Q = 0.6$ nm^{-1}. All three proteins show similar, positive values for α (Table I). From the sequences, the ratios of hydrophilic to hydrophobic residues [defined in Perkins (1986)] are similar at 50:50, 47:53, and 49:51 in that order. The similarity of the α values is thus consistent with compositional data.

(*c*) *Large-Angle Curve Analyses of C5.* Indirect transformation of the neutron curves $I(Q)$ into real space $P(r)$ using ITP (Materials and Methods) was carried out for C5, C4, C4u, and C3u to assess further the structural homologies between C3, C4, and C5. The data on C4 and C4u originated from Perkins et al. (1990). This calculation utilizes the whole scattering curve in the Q range from 0.2 to 3.4 nm^{-1}. The above R_G and R_{XS} data were based on the smaller Q range out to 0.6 nm^{-1}. Sufficient spectra for comparisons were obtained in three sessions. At large Q, the $I(Q)$ and $P(r)$ curves for C5, C4, C4u, and C3u were all similar, as illustrated for C5 and C3u in Figure 3. This agreement confirmed the structural homologies in solution to a nominal structural resolution of 1.7 nm. In Figure 3b, the maximum length of C5 and C3u was determined to be at least 15 nm and could be 18 nm from the value of r, where $P(r)$ diminishes to zero intensity. This is compatible wiith the L of 14.9–15.7 nm determined from the R_G analyses for C5. The R_G from indirect transformation was determined (Glatter, 1982) as 4.89 nm. This is in good agreement with the mean value of 4.82 ± 0.10 nm for 16 R_G values from the Guinier analyses in 100% ^2H_2O buffers (cf. the Stuhrmann plot of Figure 2a).

Table II: Comparisons of Electron Microscopy Studies on C3, C4, and C5 with the Debye Solution Scattering Model

	triaxial dimensions (nm)	reference
cobra venom factor[a]	8.2 × 13.7	Smith et al. (1982)
C4b	9 × 17	Dahlbäck et al. (1983)
C3b, C4b	6.5 × 7.5 × 12.5	Smith et al. (1984)
C5	10.4 × 14.0 × 16.8	DiScipio et al. (1983)
solution scattering model[b]		
C3, C4, C5 C3c, C4c	2 × 8 × 18	Perkins et al. (1990)
C3dg, C4d	2 × 4 × 9	

[a] The cobra venom factor is a structural analogue of C3c. The reported standard deviations are ±1.1 to ±1.3 nm. [b] See Figure 4 for the possible arrangement of the two domains.

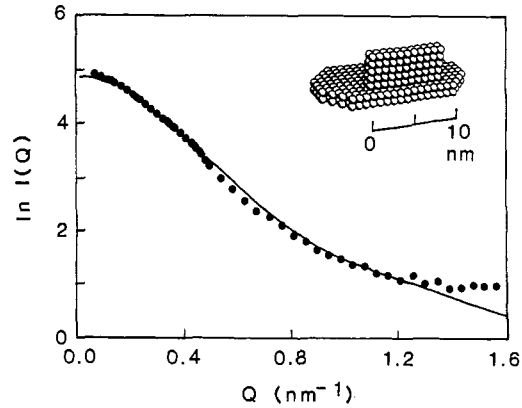

FIGURE 4: Comparison of the neutron scattering curve of C5 in ^2H_2O with Debye scattering curve simulations. The experimental data (●) are compared with the calculated Debye scattering curve (—) by using the possible two-domain model for C4 and C4u from Perkins et al. (1990). This sphere model gives a reasonable curve fit and is shown as the inset in the upper right corner. The precise arrangement of the two domains as shown should not be overinterpreted. The R_G of the model is 4.97 nm, in good agreement with the values of 4.82 and 4.89 nm from the Guinier and ITP analyses of the data in 100% ^2H_2O (see text).

A second description of the neutron curve for Q out to 1.6 nm^{-1} is obtained by computer models using Debye spheres. To test whether C5 and C4 are similar in structure, the experimental scattering curve for C5 was compared with the simulation from the C4 and C4u model (Perkins et al., 1990). The model is constructed from two distinct domains (Table II) which correspond to C4d and C4c and which are set at an angle to each other. Their dimensions are given in Table II; the length of 18 nm is slightly longer than the three calculations of 15–16 nm above but is compatible with the anticipated precision of the model. Several neutron scattering curves for C5 in 100% ^2H_2O were measured out to 1.6 nm^{-1} (cf. Figure 2b). The reasonable agreement in Figure 4 makes it likely that C5 also has a substructure with at least two domains as found for C3 and C4, even though this structure is not revealed in physiological inactivation events.

Conclusions

The scattering data from this study on C5 can be correlated with those on the homologous complement components C3 and C4 (Perkins & Sim, 1986; Perkins et al., 1990). The data of Table I show that C5 is very similar in structure to C3, C3u, C3(a+b), C4, C4u and C4(a+b). Comparisons of the full scattering curves out to a structural resolution of 2 nm (Q = 3.6 nm^{-1}) show that these three glycoproteins are structurally

closely homologous. This is fully consistent with the complete sequences that have been recently published for C3, C4, and C5 (de Bruijn & Fey, 1985; Belt et al., 1984; Wetsel et al., 1987, 1988). The comparisons of the C3, C4, and C5 sequences show that these can be readily aligned, and the location of cysteinyl residues and the hydropathy plots for C3, C4, and C5 are very similar (Nonaka et al., 1985; Wetsel et al., 1987).

This result is in contrast to previous electron microscopy studies on these complement components, as summarized in Table II (Smith et al., 1982, 1984; Dahlbäck et al., 1983). It was reported that C3, C4, and C5 possess globular structures which could be subdivided into at least two and at most four or five domains and with dimensions that differ by several nanometers. Calculation of the volume of the C3b and C4b images is comparable with values of 241 to 244 nm^3 calculated from their sequences, while that of C5 gives a volume that is 5 times larger than the sequence volume of 250 nm^3. At least one of the dimensions of C5 may be overestimated. These differences are most likely to result from the nonphysiological conditions of the measurements and perhaps magnification errors. In relation to the limited scattering data reported by Österberg et al. (1984, 1988) on C3, C4, and C5, their R_G values of C3u, C4u, and C5 were found to be similar at 5.0–5.3 nm, in agreement with our data. However, their R_G values for C3 and C4 were as low as 4.25 nm, and their α values for C3, C4, and C5 varied between -100×10^{-5} and 55×10^{-5}. These differences are best explained by the limited data that were available in these studies. For example, the range of the R_G data in Figure 2 shows that repeated measurements of the scattering curves, preferably in different buffers and protein concentrations, are necessary for a safer interpretation of the experiments.

Structural information on the three small homologous anaphylatoxins C3a, C4a, and C5a has been obtained by using protein crystallography, model building, and proton NMR (Huber et al., 1980; Greer, 1985, 1986; Nettesheim et al., 1988; Zuiderweg et al., 1988, 1989). The model building showed that C3a, C4a, and C5a all have conserved interior residues but very different external surfaces. The crystal structure of C3a has also proved to be a good model for the secondary structure of C3a and C5a in solution by NMR except at the N- and C-terminal ends of the structure. Our results extend the above observations of structural homologies.

C5 is the component upon which the membrane attack complex of complement is assembled. Since this complex is inserted into membranes, the degree to which the C5 structure is hydrophobic becomes relevant. Al Salihi et al. (1982, 1988) interpreted observations of the behavior of C5 on phenyl-Sepharose chromatography and the effects of trypsin digestion as evidence for hydrophobic surface regions on C5. Futhermore, DiScipio et al. (1983) suggested that the aggregation of C5b seen on activation of C5 was the result of the exposure of hydrophobic sites; the observation of such aggregates is supported by our preliminary neutron studies on C5b. It should, however, be noted that activation of C5 in the absence of C6 is nonphysiological and that neither C5b nor C5b6 binds to membranes. The ternary complex with C7 is required before membrane binding occurs, and it is likely that the membrane binding site of the complex lies on C7. The contrast variation data on C5 show that this has a similar internal structure to those of C3 and C4 (Table I) with hydrophilic residues found on average furthest from the core, as indeed found for globular proteins (Perkins, 1988a,b). This is to be expected since all three are water soluble and have similar ratios of hydrophobic and hydrophilic residues. The scattering data thus limit the extent to which the surface of C5 can be considered hydrophobic and, in contrast to deductions made from other biochemical investigations, rule out any significant region of surface hydrophobicity.

Acknowledgments

Dr. C. Nave and Dr. J. Torbet are thanked for generous instrumental support, Dr. O. Glatter and Dr. R. P. May are thanked for the use of the ITP and MAKITP programs, and Dr. R. A. Wetsel is thanked for the use of the human C5 sequence.

Registry No. C5, 80295-53-0; C3, 80295-41-6; C4, 80295-48-3.

References

Al Salihi, A. A., Ripoche, J., Pruvost, L., & Fontaine, M. (1982) *FEBS Lett. 150*, 238–242.

Al Salihi, A. A., Ripoche, J., & Fontaine, M. (1988) *Mol. Immunol. 25*, 367–377.

Belt, K. T., Carroll, M. C., & Porter, R. R. (1984) *Cell 36*, 907–914.

Carroll, M. C., Campbell, R. D., Bentley, P. R., & Porter, R. R. (1984) *Nature 307*, 237–241.

Dahlbäck, B., Smith, C. A., & Müller-Eberhard, H. J. (1983) *Proc. Natl. Acad. Sci. U.S.A. 80*, 3461–3465.

de Bruijn, M. H. L., & Fey, G. H. (1985) *Proc. Natl. Acad. Sci. U.S.A. 82*, 708–712.

DiScipio, R. G., Smith, C. A., Müller-Eberhard, H. J., & Hugli, T. E. (1983) *J. Biol. Chem. 258*, 10629–10636.

Ghosh, R. (1981) ILL Internal Publication 81GH29T.

Glatter, O. (1982) in *Small Angle X-Ray Scattering* (Glatter, O., & Kratky, O., Eds.) pp 119–196, Academic Press, London.

Greer, J. (1985) *Science 228*, 1055–1060.

Greer, J. (1986) *Enzyme 36*, 150–163.

Harrison, R. A., & Lachmann, P. J. (1986) Complement Technology, in *Handbook of Experimental Immunology* (Weir, D. M., Herzenberg, L. A., Blackwell, C., & Herzenberg, L. A., Eds.) pp 39.1–49, Blackwell Scientific Publications, Edinburgh.

Huber, R., Scholze, H., Pâques, E. P., & Deisenhofer, J. (1980) *Hoppe-Seyler's Z. Physiol. Chem. 361*, 1389–1399.

Law, S. K., Lichtenberg, N. A., Holcombe, F. H., & Levine, R. P. (1980) *J. Immunol. 125*, 634–639.

Nettesheim, D. G., Edalji, R. P., Mollison, K. W., Greer, J., & Zuiderweg, E. R. P. (1988) *Proc. Natl. Acad. Sci. U.S.A. 85*, 5036–5040.

Nilsson, U. R., Mandle, R. J., & McConnell-Mapes, J. A. (1975) *J. Immunol. 114*, 815–822.

Nonaka, M., Nakayama, K., Yeul, Y. D., & Takahasi, M. (1985) *J. Biol. Chem. 260*, 10936–10943.

Österberg, R., Eggertsen, G., Lundwall, A., & Sjoquist, J. (1984) *Int. J. Biol. Macromol. 6*, 195–198.

Österberg, R., Malmensten, B., Nilsson, U., Eggertsen, G., & Kjems, J. (1988) *Int. J. Biol. Macromol. 10*, 15–20.

Perkins, S. J. (1986) *Eur. J. Biochem. 157*, 169–180.

Perkins, S. J. (1988a) *Biochem. J. 254*, 313–327.

Perkins, S. J. (1988b) *New Compr. Biochem. 18B* (Part II), 143–264.

Perkins, S. J., & Weiss, H. (1983) *J. Mol. Biol. 168*, 847–866.

Perkins, S. J., & Sim, R. B. (1986) *Eur. J. Biochem. 157*, 155–168.

Perkins, S. J., Nealis, A. S., & Sim, R. B. (1990) *Biochemistry* (preceding paper in this issue).

Podack, E. R., Kolb, W. P., & Müller-Eberhard, H. J. (1978) *J. Immunol. 120*, 1841–1848.

Reid, K. B. M. (1986) *Essays Biochem. 22*, 27-68.
Smith, C. A., Vogel, C. W., & Müller-Eberhard, H. J. (1982) *J. Biol. Chem. 257*, 9879-9882.
Smith, C. A., Vogel, C. W., & Müller-Eberhard, H. J. (1984) *J. Exp. Med. 159*, 324-329.
Wetsel, R. A., Ogata, R. T., & Tack, B. F. (1987) *Biochemistry 26*, 737-743.
Wetsel, R. A., Lemons, R. S., Le Beau, M., Barnum, S. R., Noack, D., & Tack, B. F. (1988) *Biochemistry 27*, 1474-1482.
Whitehead, A. S., Soloman, E., Chambers, S., Bodmer, W. F., Povey, S., & Fey, G. (1982) *Proc. Natl. Acad. Sci. U.S.A. 79*, 5021-5025.
Zarbock, J., Gennaro, R., Romeo. D., Clore, G. M., & Gronenborn, A. M. (1988) *FEBS Lett. 238*, 289-294.
Zuiderweg, E. R. P., Henkin, J., Mollison, K. W., Carter, G. W., & Greer, J. (1988a) *Proteins: Struct., Funct. Genet. 3*, 139-145.
Zuiderweg, E. R. P., Mollison, K. W., Henkin, J., & Carter, G. W. (1988b) *Biochemistry 27*, 3568-3580.

Stereochemistry of Leukotriene B_4 Metabolites Formed by the Reductase Pathway in Porcine Polymorphonuclear Leukocytes: Inversion of Stereochemistry of the 12-Hydroxyl Group†

Sandra Wainwright,‡ J. R. Falck,§ Pendri Yadagiri,§ and William S. Powell*,‡

Endocrine Laboratory, Royal Victoria Hospital, 687 Pine Avenue West, Montreal, Quebec, Canada H3A 1A1, Department of Medicine, McGill University, Montreal, Quebec, Canada H3A 1A1, and Department of Molecular Genetics, University of Texas Southwestern Medical Center, Dallas, Texas 75235

Received June 9, 1989; Revised Manuscript Received August 21, 1989

ABSTRACT: Leukotriene B_4 (LTB_4), a potent proinflammatory agent, is a major metabolite of arachidonic acid in polymorphonuclear leukocytes (PMNL). When porcine PMNL were incubated with LTB_4 and the products purified by reversed-phase high-pressure liquid chromatography (HPLC), we previously identified two metabolites: 10,11-dihydro-LTB_4 and 10,11-dihydro-12-oxo-LTB_4 [Powell, W. S., & Gravelle, F. (1989) *J. Biol. Chem. 264*, 5364-5369]. Further analysis of the reaction products by normal-phase HPLC has now revealed the presence of a third major metabolite of LTB_4. This product is not formed in detectable amounts in the first 5 min of the reaction but accounts for about 20-30% of the reaction products after 60 min, when LTB_4 has been completely metabolized. The mass spectrum and gas chromatographic properties of the new metabolite are identical with those of 10,11-dihydro-LTB_4, suggesting that it is a stereoisomer of this compound. This product was identified as 10,11-dihydro-12-epi-LTB_4 [i.e., 5(*S*),12(*R*)-dihydroxy-6,8,14-eicosatrienoic acid] by comparison of its chromatographic properties with those of the authentic chemically synthesized compound. Both 10,11-dihydro-LTB_4 and 10,11-dihydro-12-oxo-LTB_4 were enzymatically converted to 10,11-dihydro-12-epi-LTB_4 by porcine PMNL, the former compound being the better substrate. The reaction was reversible, since both 10,11-dihydro-12-epi-LTB_4 and 10,11-dihydro-12-oxo-LTB_4 could be converted to 10,11-dihydro-LTB_4. When dihydro metabolites of LTB_4 labeled with tritium in the 12-position were incubated with porcine PMNL, only about 15% of the tritium was retained in the 12-position of the product, suggesting that epimerization due to replacement of the 12-hydroxyl group itself was unlikely. Our results would be consistent with an epimerase-catalyzed reacton in which 10,11-dihydro-12-oxo-LTB_4 is an intermediate. This would explain the lack of stereospecificity in the reduction of 10,11-dihydro-12-oxo-LTB_4 as well as the partial retention of tritium in the 12-position after epimerization. Alternatively, it is possible that the reactions could be catalyzed by a combination of stereospecific 12-hydroxy dehydrogenases and 12-keto reductases. These results indicate that the stereochemistry of 12-hydroxy eicosanoids can be reversed by PMNL, which could have important implications for their biological activities.

Leukotriene B_4 (LTB_4) is a potent mediator of inflammation which is synthesized primarily by polymorphonuclear leukocytes (PMNL)[1] (Borgeat & Samuelsson, 1979). It promotes the adhesion of leukocytes to the vascular endothelium, followed by diapedesis (Dahlén et al., 1981), and plays an important role in attracting PMNL to inflammatory sites (Higgs et al., 1981). LTB_4 is metabolized by three pathways initiated by 20-hydroxylation (Lindgren et al., 1981; Powell, 1984), 19-hydroxylation (Maas et al., 1982; Powell, 1987), and reduction to dihydro metabolites (Powell, 1987). The major route of metabolism of LTB_4 in human PMNL is the LTB_4 20-hydroxylase pathway (Lindgren et al., 1981; Powell, 1984), resulting in the formation of 20-hydroxy-LTB_4 and subsequently 20-oxo-LTB_4 and ω-carboxy-LTB_4 (Soberman et al.,

† This work was supported by grants from the Medical Research Council of Canada (W.S.P.) and the National Institutes of Health (J.R.F.). S.W. was supported by a studentship award from the Medical Research Council of Canada.

* Correspondence should be addressed to this author at the Royal Victoria Hospital.
‡ Royal Victoria Hospital and McGill University.
§ University of Texas Southwestern Medical Center.

[1] Abbreviations: LT, leukotriene, 12-HETE, 12-hydroxy-5,8,10,14-eicosatetraenoic acid; RP-HPLC, reversed-phase high-pressure liquid chromatography; NP-HPLC, normal-phase high-pressure liquid chromatography; ODS, octadecylsilyl; GC-MS, gas chromatography-mass spectrometry; PMNL, polymorphonuclear leukocytes.

0006-2960/90/0429-1180$02.50/0